

Towards Scalable Gaussian Process Modeling

Piyush Pandita*, Jesper Kristensen, Liping Wang

Probabilistics and Optimization Team, GE Research, Niskayuna, New York, 12309

* piyush.pandita@ge.com

Abstract

Numerous engineering problems of interest to the industry are often characterized by expensive black-box objective function evaluations. These objective functions could be physical experiments or computer simulations. Obtaining a comprehensive idea of the problem and/or performing subsequent optimizations generally requires hundreds of thousands of evaluations of the objective function which is most often a practically unachievable task. Gaussian Process (GP) surrogate modeling replaces the expensive function with a cheap-to-evaluate data-driven probabilistic model. While the GP does not assume a functional form of the problem, it is defined by a set of parameters, called hyperparameters, that need to be learned from the data. The hyperparameters define the characteristics of the objective function, such as smoothness, magnitude, periodicity, etc. Accurately estimating these hyperparameters is a key ingredient in developing a reliable and generalizable surrogate model. Markov chain Monte Carlo (MCMC) is a ubiquitously used Bayesian method to estimate these hyperparameters. At GE's Global Research Center, a customized industry-strength Bayesian hybrid modeling framework utilizing the GP, called GEBHM, has been employed and validated over many years. GEBHM is very effective on problems of small and medium size, typically less than 1000 training points. However, the GP does not scale well in time with a growing dataset and problem dimensionality which can be a major impediment in such problems. For some challenging industry applications, the predictive capability of the GP is required but each second during the training of the GP costs thousands of dollars. In this work, we apply a scalable MCMC-based methodology enabling the modeling of large-scale industry problems. Towards this, we extend and implement in GEBHM an Adaptive Sequential Monte Carlo (ASMC) methodology for training the GP. This implementation saves computational time (especially for large-scale problems) while not sacrificing predictability over the current MCMC implementation. We demonstrate the effectiveness and accuracy of GEBHM with ASMC on four mathematical problems and on two challenging industry applications of varying complexity.

Keywords: Surrogate modeling, Bayesian inference, Sequential Monte Carlo, Gaussian Processes, Design under uncertainty

1 Introduction

Computer simulators [35] and/or sophisticated in-house laboratory experiments [10] representing physical phenomena generally pose the problem of being computationally or logistically challenging. In scenarios where extracting information [21, 26] about an underlying physical process to forecast or predict its behaviour is critical, generating hundreds of thousands of experimental data points becomes infeasible. To alleviate the above issue, surrogate modeling (also called predictive modeling) is a popular approach towards obtaining an inexpensive representation of the simulation or experiment.

Among the myriad surrogate modeling [18] techniques, Gaussian Process (GP) [37] regression (GPR) is a well established technique in the area of probabilistic modeling

of expensive functions. GPR is a non-parametric machine learning technique in the sense that it does not make assumptions about the functional form of the function being modeled. However, the GP model does have parameters, called hyperparameters, that capture characteristics such as periodicity, smoothness, measurement noise, etc., of the underlying function. These hyperparameters are learned from the data (limited set of observations) using empirical Bayesian techniques like maximum likelihood estimation [31], or fully Bayesian [22] methods based on Markov chain Monte Carlo (MCMC) [34, 11]. For a typical GP the number of hyperparameters is on the order of 10-100. Furthermore, the predictive accuracy of the GP is highly sensitive to the values of the hyperparameters thus requiring sophisticated optimization. The high dimensionality of the hyperparameter space prompts a rigorous MCMC treatment [7] to learn the hyperparameters. Also, the Bayesian MCMC [15, 6, 17] methods allow quantification of uncertainties [13] around the estimates of the hyperparameters, which makes possible drawing samples from the space of the underlying function.

Recent work on extending GPs to big-data applications has focused on deriving variational representations of GPs [32], constructing sparse approximations of GPs [20, 33] and training local GPs using informative subsets of the data [36, 27]. However, for most of these methods, the modeling assumes the parameters of the covariance kernel fixed to point estimates that are obtained using optimization or are considered known. A recent review of methods for extending GPs for big-data applications can be found in [29]. In this paper, we restrict our focus to Bayesian GPs where the covariance parameters are inferred using MCMC.

GE’s Global Research Center has its own implementation of fully Bayesian modeling, called GE Bayesian Hybrid Modeling (GEBHM), which has been applied [14, 25] successfully to various engineering problems over many years. Given the greater predictability achieved by using MCMC, the MCMC method comes with its own pitfalls [30]. For example, in problems involving huge training data sets, on the order of $N = 1000$ data points, the excessive computational training time is a direct consequence of a large number of GP covariance matrix inversion operations, scaling as $O(N^3)$. The work done in [28] has focused on circumventing this problem by obtaining approximations to the inverse of the matrix. Scalability of the MCMC methods with varying complexity of the problem, such as increasing number of input dimensions [19], multiple correlated functions, etc., can break down when applied to challenging industrial problems.

Sequential Monte Carlo (SMC) [9, 8] methods offer a promising alternative considering the availability of multiple individual processor elements (PEs), also called cores, and high performance computing environments. The inherent parallelizability paves the way for SMC methods to be used in fitting the hyperparameters through a form of importance sampling and reduce the required number of matrix inversions per PE. Moreover, SMC methods can be tweaked by the user based on the type of problem through multiple *knobs* which determine characteristics of the SMC such as number of simultaneously running MCMC chains, number of MCMC steps per chain, discretization of the posterior distribution into finite samples, etc. This magnanimity is an innate feature of most SMC algorithms [2, 1], the theory of which guarantees convergence under specific assumptions [4, 3]. We apply an adaptive SMC (ASMC) method [23], by leveraging *pySMC* (a package written in the PYTHON programming language). The details of the *pySMC* library are provided at <https://github.com/ebillionis/pysmc>. The ASMC method samples according to the same kernel as GEBHM’s standard MCMC, albeit reducing the number of covariance matrix inverse computations by an order of magnitude. This difference is critical to the ASMC alleviating the burden of excessive computational time in GP model training. We extend the capabilities and flexibility of the ASMC by allowing for a predefined set of importance sampling distributions which could be provided by the user, based on the complexity of the problem. As an addendum to the methodology,

fine-tuning of the widths of proposal distributions of the hyperparameters is done on the fly, independently.

The purpose of this study is to verify the scalability of ASMC, its higher predictive accuracy, and to demonstrate the savings in time (which translate to cost savings) that can be leveraged henceforth. The investigation is carried out using six problems with varying types of complexity in terms of the input dimensionality, the number of outputs, the size of the training data, etc. The comparison tests are done using multiple PEs on a workstation computer to highlight the ease of implementation and usability of the ASMC. Further comparison tests include the results obtained by the seamless scalability achieved by ASMC using high performance computing (HPC) clusters. Out of the six chosen problems four are synthetic in nature with different dimensionality and training data size and two stem from GE industrial applications.

The outline of the paper is as follows. We start Sec. 2 by providing some basic mathematical definitions of GPR and the details of the posterior of the hyperparameters of the GP. Our numerical results are presented in Sec. 3. The impact of the ASMC on problems with large training data sets is highlighted in Sec. 3.1. In particular, in Sec. 3.3, Sec. 3.4 and Sec. 3.5, we validate our approach using three synthetic problems with varying input dimensionality. In Sec. 4.1 and Sec. 4.2, we apply the ASMC methodology to solve a challenging steam turbine compressor problem and a multi-objective combustion problem, respectively. We present our conclusions in Sec. 5.

2 Methodology

2.1 Gaussian process regression

The surrogate models that GEBHM builds for the overall objective(s) for the problem are data-driven statistical models that rely on the Bayesian nature of GPR [37]. GPs are non-parametric meaning, they do not assume a model form (think: polynomial of degree n , among others). GPs try to map inputs to outputs by superposing several Gaussian distribution functions. GPs can accurately model complex variations in the data, they can capture discontinuities effectively and can produce very accurate surrogate statistical models with comparatively less data. An important feature is that GPs offer a measure of the quality of the surrogate statistical model and direct us to areas of input space where we need more data, for example [24]. We now go over the finer details of GPR where we define the posterior distribution of the hyperparameters which we want to sample from. We use a zero mean for the GP. The covariance of the GP is computed based on a kernel that is a function of the distance between the inputs. For a multi-objective problem the covariance matrix is a block diagonal matrix comprising of the individual covariance matrices for each of the objectives. The covariance for an m output, d input, problem with N training data points is shown below:

$$\Sigma = \begin{bmatrix} \Sigma^{(1)} & & \\ & \ddots & \\ & & \Sigma^{(m)} \end{bmatrix}, \quad (1)$$

where each of the individual elements along the diagonal represent the covariance matrix of dimension $N \times N$ of a single output. These can be more generally expressed as in Eq. (2).

$$\Sigma_{ij}^{(k)} = \frac{1}{\lambda_z^{(k)}} \sum_{l=1}^d \exp \left[-\beta_l^{(k)} (x_{i,l} - x_{j,l})^2 \right] + I \frac{1}{\lambda_s^{(k)}} + I \frac{1}{\lambda_o} \quad (2)$$

where $i, j \in \{1, \dots, N\}$, $k \in \{1, \dots, m\}$, $l \in \{1, \dots, d\}$, $x_{i,l}$ is the value of the i th training point in the l th input dimension, and let $\beta^{(k)} = \{\beta_1^{(k)} \dots \beta_d^{(k)}\}$. The hyperparameters

of the GP model are $\boldsymbol{\theta} = \{\boldsymbol{\beta}^{(k)}, \lambda_z^{(k)}, \lambda_s^{(k)}, \lambda_o\}_{k=1}^m$. The $\boldsymbol{\beta}^{(k)}$ parameters represent the inverted length-scales of the covariance kernel. $\lambda_z^{(k)}$ is also called the signal-strength which is proportional to the scale of the magnitude for the objective space and $\lambda_s^{(k)}$ represents the precision of the random Gaussian measurement noise. λ_o represents the precision of the random Gaussian measurement noise to account for the overall randomness between the multiple outputs. It can be inferred from above that for our problems of learning the model’s hyperparameters, it is always a problem of estimating $m \times (d + 2) + 1$ number of parameters. The likelihood of observing the training data for a selected set $\boldsymbol{\theta}$ of hyperparameters is:

$$L(\mathbf{Y}|\boldsymbol{\theta}) = \frac{1}{|\Sigma|^{\frac{1}{2}}} \exp\left(-\frac{1}{2}\mathbf{Y}^T \Sigma^{-1} \mathbf{Y}\right), \quad (3)$$

where the i, j th element of the matrix \mathbf{Y} is the j th output value for the i th training data point. The conditional posterior of the hyperparameter set $\boldsymbol{\theta}$ can be written as follows:

$$p(\boldsymbol{\theta}|\mathbf{Y}) \propto L(\mathbf{Y}|\boldsymbol{\theta})p(\lambda_o) \prod_{k=1}^m p(\boldsymbol{\beta}^{(k)})p(\lambda_z^{(k)})p(\lambda_s^{(k)}). \quad (4)$$

The posterior given in Eq. (4) is the so-called *target distribution* known only up to a proportionality constant. The sequence of sampling distributions in the ASMC are derived from the functional form given in Eq. (4).

2.2 MCMC in GEBHM

The implementation of MCMC in GEBHM works in two phases: a) the initialization phase and b) the main chain. The initialization phase of the MCMC solves the purpose of selecting the proposal width of the proposal distributions for the main (full) chain of the MCMC. This initialization process can only be performed on a single PE, thus limiting the computational power offered by multiple cores. The main chain can use multiple cores, but the single core operation of initialization does contribute to a significant percentage of the total cost of the MCMC in GEBHM. The complete details of the initialization process have been omitted to protect company proprietary information. The MCMC algorithm uses a Metropolis algorithm [12] for making jumps (steps) during the main chain.

2.3 Adaptive sequential Monte Carlo

The sequential Monte Carlo methodology (also known as particle filtering in some literature) [16] essentially uses a coherent sequence of distributions to do MCMC sampling from. This sequence of distributions starts with a distribution mimicking a uniform distribution and progressively moves closer (in analytical form) to the posterior distribution Eq. (4) (in our case). A sequence of n sampling distributions based on the empirical form given in Eq. (7) can be built with $\gamma_0 \sim 0$ and $\gamma_n = 1$. Thus, the sampling process can be understood as a slow progression from a non-informative *uniform* distribution to the target posterior distribution Eq. (4). The jumps between states for all sampling distributions are based on a Metropolis stepper (same as the one being used for MCMC in GEBHM). The conditional posterior in Eq. (4) is reproduced in Eq. (5) while we shun the dependence on \mathbf{Y} to clearly represent the form of the sampling distributions of the ASMC as a function of only the hyperparameters $\boldsymbol{\theta}$. The sampling distributions are illustrated in Eq. (6). Each $p_i(\boldsymbol{\theta})$ is a sampling distribution and each chain (ASMC

particle) takes num_{asmc} steps before moving on to a different value of γ .

$$p(\boldsymbol{\theta}) \propto \pi(\boldsymbol{\theta}) \quad (5)$$

$$p_i(\boldsymbol{\theta}) \propto \pi_i(\boldsymbol{\theta}) \quad (6)$$

$$\pi_i(\boldsymbol{\theta}) = \pi(\boldsymbol{\theta})^{\gamma_i}. \quad (7)$$

At each γ_i the corresponding distribution $p_i(\boldsymbol{\theta})$ is described as a discrete particle approximation as shown in Eq. (8).

$$p_i(\boldsymbol{\theta}) \approx \sum_{j=1}^N w^{j_i} \delta(\boldsymbol{\theta} - \boldsymbol{\theta}^{j_i}) \quad (8)$$

These finite number of samples are called particles (parallel MCMC chains). At each value of γ each particle takes a predefined number of steps num_{asmc} . Thus, each particle evolves its own MCMC chain based on the Metropolis stepper. The values of γ visited by the algorithm are governed by a statistic known as the *effective sample size* (*ess*). The *ess* is calculated as defined in Eq. (9). Thus, when all particles have equal weights the *ess* is equal to the number of particles, N . The *ess* guides the methodology finding the next γ i.e. γ_{i+1} as shown in Eq. (9).

$$ess|\gamma_i = \sum_{j=1}^N \frac{1}{w^{j_i}{}^2} \quad (9)$$

$$ess|\gamma_{i+1} = ess_reduction \times ess|\gamma_t, \quad (10)$$

where *ess_{reduction}* is a predefined threshold $\in (0, 1)$. The γ_{i+1} is usually selected via an algorithm like [5]. For more details on the *ess* and the selection of γ_{i+1} the reader is referred to the work of [3, 4]. The dynamic selection of the set of γ s for a single ASMC requires special attention in the industrial context. For some problems the dynamic selection process can be too time consuming. Towards ameliorating this we replace the dynamic selection of the γ parameter with a prespecified set of γ s called the *grid*. The *grid* used in this works allows uniform sized jumps for the γ parameter but we expect better results with a non-uniform *grid*. Consider Eq. (10), the number of γ s visited by the ASMC can vary based on factors such as the size of training data, number of input dimensions, etc. The *grid* thus constrains the freedom of the algorithm especially when time is a greater priority for a user than small gains in accuracy. We list the steps taken by GEBHM's ASMC methodology in algorithm 1. The added advantage of the ASMC

Algorithm 1 ASMC in GEBHM.

Require: number of steps per particle num_{asmc} , *grid*: γ , MCMC stepper,

- 1: Initialize the particles (chains) via MCMC stepper.
 - 2: **for** $i \in [1, n]$ **do**
 - 3: Do num_{asmc} steps for each particle.
 - 4: *tune* the proposal widths of the proposal distributions for each hyperparameter based on the respective acceptance ratios from the MCMC stepper.
 - 5: $\gamma \leftarrow \gamma_i$
 - 6: **end for**
-

is the lack of need to pre-compute the proposal widths (as is the case for MCMC in GEBHM) as it adaptively scales the proposal widths on the fly for each parameter. The exploration of posteriors of parameters with multiple modes is a problem that the ASMC is semantically designed to tackle.

3 Results

We first present our numerical results demonstrating the ASMC’s ability to scale well with large training data sets.

3.1 Toy problem 1: Scalability

As mentioned in Sec. 1, the standard MCMC implementation makes the GP model training process cumbersome. In cases with large training data, the aforementioned problem worsens with the whole data set not being put to use for training the GP model. Reducing the frequency of the computationally challenging part is critical to the consequence of applying a MCMC method to GP model training. We apply the ASMC to the following 10 dimensional non-linear mathematical problem:

$$y(\mathbf{x}) = 3 \sin(x_1)x_2 + \cos(x_3) \sin(x_4) + \sin(x_5) \sin(x_6) + \sin(x_7) + \sin(x_8) + 7x_9 + 6x_{10} \quad (11)$$

Eq. (11) enables us to generate a large training data set (greater than 1000 points). The performance of the two algorithms, GEBHM and ASMC, is highlighted in Fig. 1 (a), (b) and (c). ASMC’s ability to handle large sets of data is clearly visible in Fig. 1 (a) where the standard MCMC takes almost four times as long as the ASMC with around 1000 training data points. Secondly, the ASMC’s GP model building times are comparatively low even with training data size greater than 3000 points. This is accomplished due to ASMC’s seamless operational scalability to HPC environments. Fig. 1 (b) highlights the predictive accuracy achieved by ASMC (which is mainly a satisficing objective) being equal to or better than the standard MCMC. The MCMC settings were kept at 6800 steps including 2000 steps for the initialization phase. The savings in absolute time shown in Fig. 1(c) provide an idea of the potential improvement made by using ASMC for GP model building with high training data problems. It is important to consider the non-parallelizability of the initialization (shown in purple) of the MCMC, which limits the depth of impact that can be achieved by using a larger number of cores (greater than 12) for the GEBHM. The times represented by the initialization will remain fixed irrespective of the number of cores, thus making the comparison with ASMC even more realistic. For the scalability problem we allow the ASMC to identify the set of sampling distributions on the fly, see Eq. (10), hence not specifying the *grid*.

3.2 ASMC and MCMC settings

Now, we move on to the comparison of the ASMC with GEBHM’s MCMC on three synthetic problems. We plot the RMSE for the ASMC obtained using the final particle approximation for different number of particles, keeping the number of cores on a workstation fixed. As the number of particles increases, the time taken to build the GP model also increases and the corresponding RMSE shows gradual decrease. This is done because plotting the RMSE by using particles from the different sampling distributions of a single ASMC run would be misleading simply because the sampling distributions visited by the ASMC are different from one another. This is a crucial step, where the ASMC differs from the conventional MCMC (where the sampling distribution remains the same i.e. the posterior distribution of the hyperparameters known up to a proportionality constant Eq. (4)).

For workstation computations the ASMC settings are fixed to 6 cores, and the number of particles at 6, 12, 30, and 60. For HPC computations we vary the number of cores and fix the number of particles equal to the number of cores for each run of the ASMC. The number of cores for the HPC runs of the ASMC for all problems are 24, 48, 120,

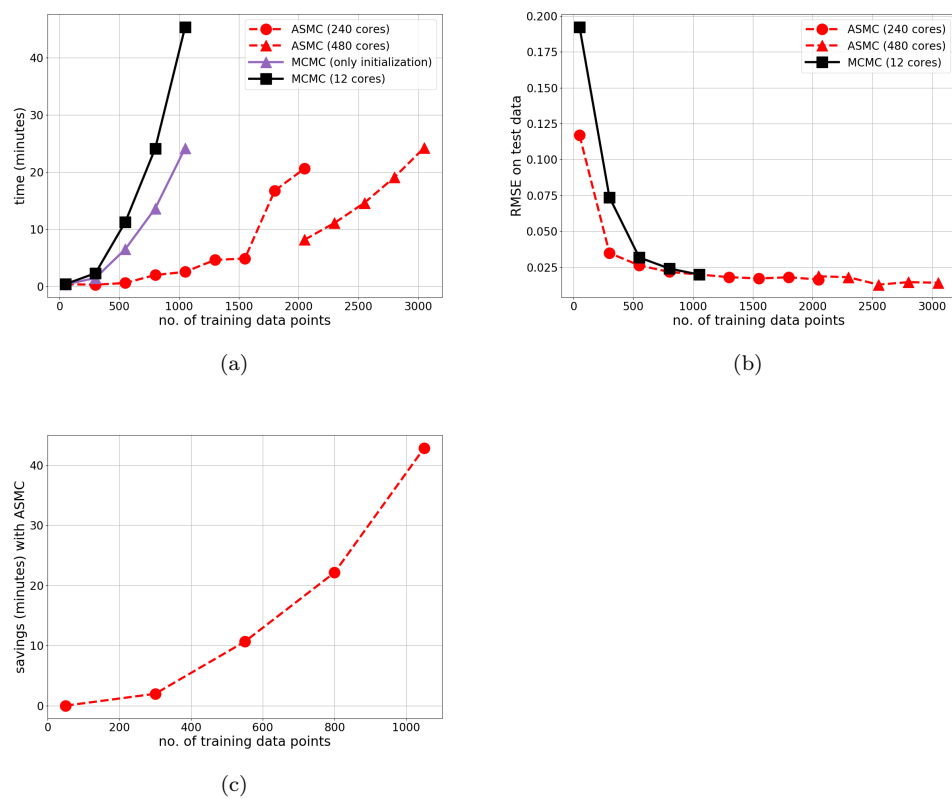


Figure 1: Subfigures (a), (b) and (c) show the scalability, predictive accuracy and savings in time for the ASMC compared to MCMC for a large training data set problem respectively. The number of particles for the ASMC is 480, for all runs.

240, and 480. For ASMCs performance on the HPC with greater than 480 particles (for the toy problem in Sec. 3.5), the number of cores is fixed at 480 (the highest number available during our experiments on the HPC).

However, for the standard MCMC, the RMSE on the test data is plotted against time as the chains evolve. The settings for the standard MCMC are 5800 steps including 1000 steps for initialization. The γ_0 values are 0.001 and 0.00001 for the ASMC’s runs on the workstation and the HPC, respectively.

3.3 Toy problem 2

The four dimensional problem, is a single-objective problem with a known analytic form of the objective. The objective function is a quadratic function of the four input variables. For safeguarding proprietary information of GE’s business partners, the full functional form of the input-output relation has been omitted from the text.

The purpose of comparing the two algorithms on a low-dimensional problem is to

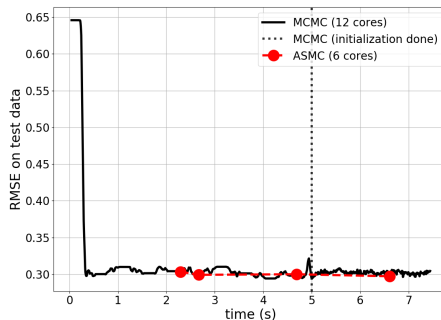


Figure 2: Root mean squared error versus time taken to build the GP model for the two algorithms for the four dimensional toy problem. Number of particles (red dots) are 6, 12, 30, and 60, across the time axis for ASMC.

demonstrate the ability of the ASMC to replace the standard MCMC on a workstation, before showing comparisons between the two methodologies by leveraging HPC platforms. Fig. 2 shows the savings in time on a workstation with the ASMC using 6 cores and the GEBHM standard MCMC using 12 cores after the completion of the initialization (done on a single core). Each red dot in Fig. 2 represents the RMSE on test data after the completion of the ASMC GP model building, as the number of particles for the ASMC is varied across time. For the standard MCMC, the RMSE on test data during initialization is separated from the rest of the particles by the vertical dotted line. The standard MCMC RMSE versus time is plotted by computing the RMSE at each time step of the MCMC chain. Higher dimensional problems are used to compare the two algorithms with ASMC scaled-up on the HPC. The number of steps per ASMC particle is equal to one. The *grid* is fixed at 10 steps and 20 steps for the workstation and HPC, respectively.

3.4 Toy problem 3

We use an 18 dimensional, single-objective problem to further demonstrate the effectiveness of the methodology. The problem is a torsion vibration problem where the high natural frequency of a three-shaft and two-disk system is the objective function. The input variables include the diameter, length, rigidity and weight density of the three shafts

and the diameter, thickness, weight density of the two disks. A diagram representing the structure of the system is shown in Fig. 3. The problem can be mathematically represented as follows:

$$\begin{aligned}
 y &= \frac{\sqrt{\frac{-b + \sqrt{b^2 - 4ac}}{2a}}}{2\pi} \\
 a &= 1 \\
 b &= -\left(\frac{K_1 + K_2}{J_1} + \frac{K_2 + K_3}{J_2}\right) \\
 c &= \frac{K_1 K_2 + K_2 K_3 + K_3 K_1}{J_1 J_2}
 \end{aligned}$$

where,

$$\begin{aligned}
 K_i &= \frac{\pi G_i d_i}{32 L_i} \\
 M_j &= \frac{\pi t_j \rho_j D_j}{4g} \\
 J_j &= \frac{1}{2} M_j \left(\frac{D_j}{2}\right)^2
 \end{aligned} \tag{12}$$

for $i \in \{1, 2, 3\}$ and $j \in \{1, 2\}$. The d_i s, L_i s, G_i s and λ_i s represent the diameter, length, rigidity and the weight density of the three shafts and D_j s, t_j s and ρ_j s represent the diameter, thickness, and weight density of the two disks, respectively.

The convergence analysis of the two algorithms is shown in Fig. 4. The number of steps per ASMC particle is five. The *grid* is fixed at 10 steps and 20 steps for the workstation and HPC, respectively.

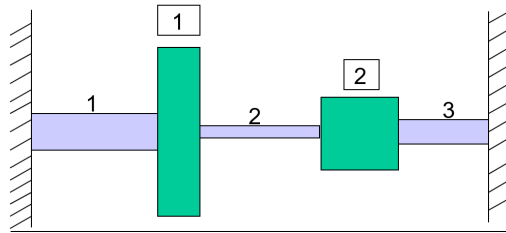


Figure 3: The setup of the torsion vibration problem.

3.5 Toy problem 4

A 100 dimensional non-linear single-objective problem poses a strong challenge in terms of the number of input dimensions to test the performance of both methodologies. The explicit details of the functional relationship have been omitted from the manuscript.

The convergence in terms of the RMSE on test data as a function of time is shown in Fig. 5. The convergence for the workstation based runs can be seen in Fig. 5 (a), where the ASMC reaches almost similar accuracy as the standard MCMC in less than half the time (with 30 particles). Similar convergence trends can be seen for the ASMCs runs on the HPC with varying number of particles (24, 48, 240, 480, 960 and 2400) with time. The number of steps taken by each ASMC particle is one for both (workstation and HPC) cases. The *grid* is fixed at 10 steps and 20 steps for the workstation and HPC,

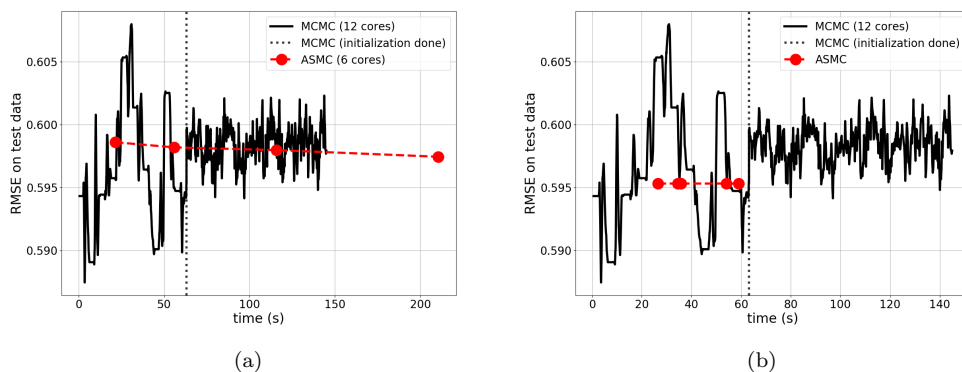


Figure 4: Subfigure (a) Number of particles on a workstation (red dots) are 6, 12, 30, and 60, and Subfigure (b) number of particles on the HPC (red dots) are 24, 48, 120, 240, and 480, across the time axis, respectively for the torsion problem.

respectively. The finer *grid* considered for the HPC is to gain greater predictive accuracy while relying on the HPC (large number of cores) to compensate for the computational overheads incurred.

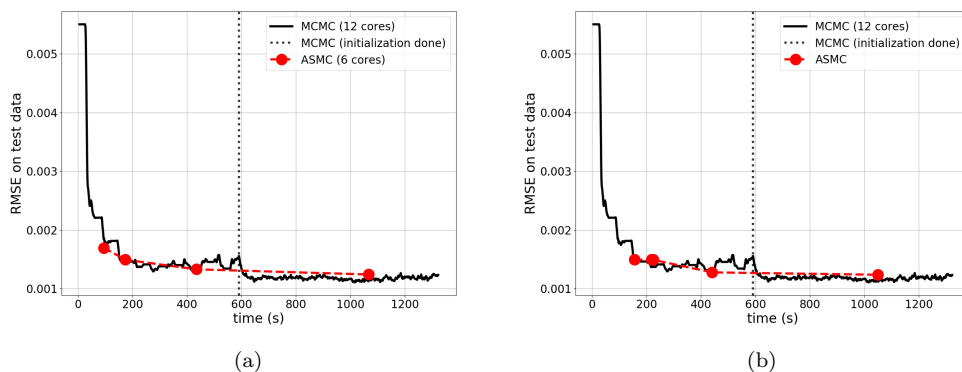


Figure 5: Subfigure (a) Number of particles on a workstation (red dots) are 6, 12, 30, and 60, and Subfigure (b) number of particles on the HPC (red dots) are 48, 240, 480, 960 and 2400, across the time axis, respectively for the 100 dimensional problem.

4 Industry problems

4.1 Steam turbine compressor problem

This is a five dimensional, single-objective design optimization problem, where the training data set is observed from temperature experiments. The goal is to obtain the best system design given requirements on the temperature distributions. The number of steps taken by the ASMC particles during the workstation based runs is five and for the runs on the HPC is one. The *grid* is fixed at 10 steps for both, workstation and HPC. The savings in time and, for this case noticeable, gains in predictive accuracy are shown in Fig. 6. Not only does the ASMC show explicit time savings, but with the HPC it also results in

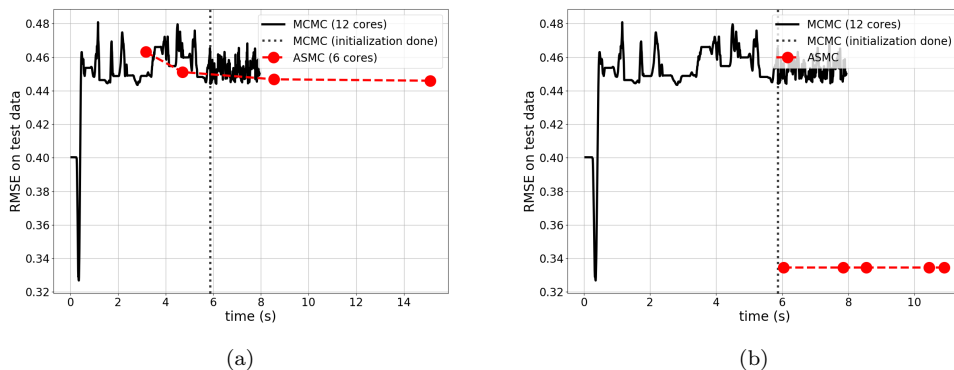


Figure 6: Subfigure (a) Number of particles on a workstation (red dots) are 6, 12, 30, and 60, and Subfigure (b) number of particles on the HPC (red dots) are 24, 48, 120, 240, and 480, across the time axis, respectively for the steam turbine compressor problem.

greater predictive accuracy than the GEBHM standard MCMC as shown in Fig. 6 (b). This indicates the dense representation of the sampling distributions made possible by using the HPC (where each particle runs on a separate core).

4.2 Combustion problem

The problem is a GE combustion test data problem, where we aim to build a GP model to predict two emission quantities as a function of three measured temperatures, three fuel flow parameters, and air flow. Thus, there are 9 hyperparameters that need to be estimated for each individual objective. The total number of hyperparameters for the GP model is 19. The MCMC settings for this problem are: 10000 steps with 1000 steps during the initialization. The significance of the results in Fig. 7 and Fig. 8 is noticeable

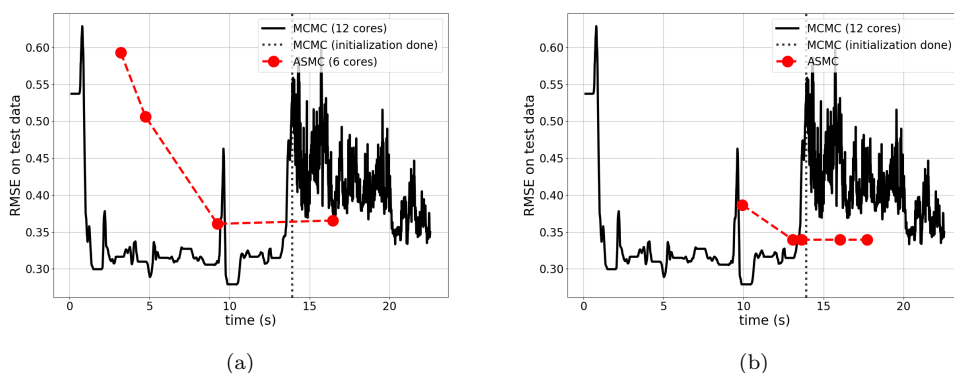


Figure 7: Subfigure (a) Number of particles on a workstation (red dots) are 6, 12, 30, and 60, and Subfigure (b) number of particles on the HPC (red dots) are 24, 48, 120, 240, and 480, across the time axis, respectively for the first objective of the combustion problem.

from the perspective of the number of objectives. Not only does the scaled-up HPC ASMC do well in terms of computational time but it improves the predictive accuracy of

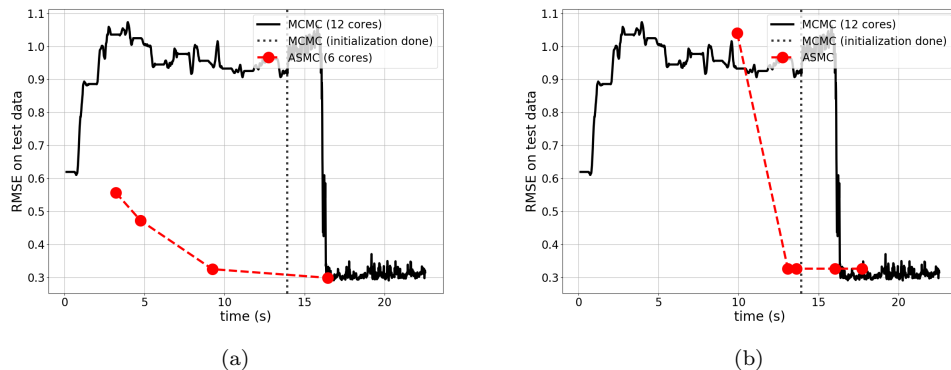


Figure 8: Subfigure (a) Number of particles on a workstation (red dots) are 6, 12, 30, and 60, and Subfigure (b) number of particles on the HPC (red dots) are 24, 48, 120, 240, and 480, across the time axis, respectively for the second objective of the combustion problem.

the GP model compared to GEBHM’s MCMC. The number of steps per ASMC particle is one for the workstation and five for the HPC runs. The *grid* is fixed at 10 steps for both computing environments.

This provides a holistic overview of ASMC’s performance on different types of problems. Problems of varying input dimensionality, varying number of objectives, and different training data sizes have been treated with the extended ASMC and compared to the current MCMC implementation. The ASMC does equally well or better compared to the MCMC in terms of predictive accuracy, while saving time by half or more in most of the challenging problems.

5 Conclusions

We demonstrate the working of the implementation of an ASMC method in GEBHM, and compare it to the performance of the existing semi-parallelizable MCMC algorithm on mathematical problems and challenging industrial problems with varying complexity. The main reason behind leveraging ASMC is the inherent flexibility and scalability offered by the algorithm’s parallelizable nature, which is practically implementable with the availability of *high-end* computational resources such as HPCs. The numerical results on toy problems of different input dimensionality show the versatility of the extended ASMC on both, workstation and HPC environments. This is augmented by extending the flexibility of the ASMC to allow the user to prespecify the sequence of sampling distributions. Thus, allowing the algorithm to balance savings in time and predictive accuracy. It is interesting to note that the ASMC has the inherent capability to treat different problems differently, but can also almost always perform well with a reasonable setting of the default parameters. The different parameters chosen with different problems in Sec. 3 further highlights this nuance of the ASMC. ASMC’s performance on the combustion data problem, demonstrates its ability to perform equally well with multiple objectives. Future directions of work on studying the algorithm include determining an optimal set of parameter settings for an arbitrary problem. This is important from the perspective of making the ASMC’s implementation deliverable to users averse to the flexibility of the ASMC.

6 Acknowledgements

The authors wholeheartedly thank Dr. Ilias Bilonis, Purdue University for providing technical insights into this research.

References

- [1] C. Andrieu, A. Doucet, and R. Holenstein. Particle markov chain monte carlo methods. *Journal of the Royal Statistical Society: Series B (Statistical Methodology)*, 72(3):269–342, 2010.
- [2] C. Andrieu, A. Doucet, and E. Punskeya. Sequential monte carlo methods for optimal filtering. In *Sequential Monte Carlo Methods in Practice*, pages 79–95. Springer, 2001.
- [3] I. Bilonis, B. A. Drewniak, and E. M. Constantinescu. Crop physiology calibration in the clm. *Geoscientific Model Development*, 8(4):1071–1083, 2015.
- [4] I. Bilonis and P.-S. Koutsourelakis. Free energy computations by minimization of kullback–leibler divergence: An efficient adaptive biasing potential method for sparse representations. *Journal of Computational Physics*, 231(9):3849–3870, 2012.
- [5] R. P. Brent. An improved monte carlo factorization algorithm. *BIT Numerical Mathematics*, 20(2):176–184, 1980.
- [6] C. M. Carlo. Markov chain monte carlo and gibbs sampling. *Lecture notes for EEB*, 581, 2004.
- [7] M. K. Cowles and B. P. Carlin. Markov chain monte carlo convergence diagnostics: a comparative review. *Journal of the American Statistical Association*, 91(434):883–904, 1996.
- [8] P. Diaconis. *Sequential monte carlo methods in practice*, 2003.
- [9] A. Doucet, N. De Freitas, and N. Gordon. An introduction to sequential monte carlo methods. In *Sequential Monte Carlo methods in practice*, pages 3–14. Springer, 2001.
- [10] N. Flournoy. A clinical experiment in bone marrow transplantation: Estimating a percentage point of a quantal response curve. In *case studies in Bayesian Statistics*, pages 324–336. Springer, 1993.
- [11] A. Gelman, J. B. Carlin, H. S. Stern, and D. B. Rubin. *Bayesian data analysis*. Chapman and Hall/CRC, 1995.
- [12] A. Gelman, G. O. Roberts, W. R. Gilks, et al. Efficient metropolis jumping rules. *Bayesian statistics*, 5(599-608):42, 1996.
- [13] Z. Ghahramani and C. E. Rasmussen. Bayesian monte carlo. In *Advances in neural information processing systems*, pages 505–512, 2003.
- [14] S. Ghosh, I. Asher, J. Kristensen, Y. Ling, K. Ryan, and L. Wang. Bayesian multi-source modeling with legacy data. In *2018 AIAA Non-Deterministic Approaches Conference*, page 1663, 2018.
- [15] W. R. Gilks, S. Richardson, and D. Spiegelhalter. *Markov chain Monte Carlo in practice*. CRC press, 1995.

- [16] N. J. Gordon, D. J. Salmond, and A. F. Smith. Novel approach to nonlinear/non-gaussian bayesian state estimation. In *IEE Proceedings F (Radar and Signal Processing)*, volume 140, pages 107–113. IET, 1993.
- [17] P. J. Green. Reversible jump markov chain monte carlo computation and bayesian model determination. *Biometrika*, 82(4):711–732, 1995.
- [18] R. F. Gunst. Response surface methodology: process and product optimization using designed experiments, 1996.
- [19] H. Haario, M. Laine, M. Lehtinen, E. Saksman, and J. Tamminen. Markov chain monte carlo methods for high dimensional inversion in remote sensing. *Journal of the Royal Statistical Society: series B (statistical methodology)*, 66(3):591–607, 2004.
- [20] J. Hensman, N. Fusi, and N. D. Lawrence. Gaussian processes for big data. *arXiv preprint arXiv:1309.6835*, 2013.
- [21] E. T. Jaynes. Information theory and statistical mechanics. *Physical review*, 106(4):620, 1957.
- [22] M. C. Kennedy and A. O’Hagan. Bayesian calibration of computer models. *Journal of the Royal Statistical Society: Series B (Statistical Methodology)*, 63(3):425–464, 2001.
- [23] J. Kristensen, I. Bilonis, and N. Zabaras. Relative entropy as model selection tool in cluster expansions. *Physical Review B*, 87(17):174112, 2013.
- [24] J. Kristensen, I. Bilonis, and N. Zabaras. Adaptive simulation selection for the discovery of the ground state line of binary alloys with a limited computational budget. In *Recent Progress and Modern Challenges in Applied Mathematics, Modeling and Computational Science*, pages 185–211. Springer, 2017.
- [25] J. Kristensen, Y. Ling, I. Asher, and L. Wang. Expected-improvement-based methods for adaptive sampling in multi-objective optimization problems. In *ASME 2016 International Design Engineering Technical Conferences and Computers and Information in Engineering Conference*, pages V02BT03A024–V02BT03A024. American Society of Mechanical Engineers, 2016.
- [26] S. Kullback. *Information theory and statistics*. Courier Corporation, 1997.
- [27] B.-J. Lee, J. Lee, and K.-E. Kim. Hierarchically-partitioned gaussian process approximation. In *Artificial Intelligence and Statistics*, pages 822–831, 2017.
- [28] W. E. Leithead and Y. Zhang. O (n²)-operation approximation of covariance matrix inverse in gaussian process regression based on quasi-newton bfgs method. *Communications in Statistics—Simulation and Computation*®, 36(2):367–380, 2007.
- [29] H. Liu, Y.-S. Ong, X. Shen, and J. Cai. When gaussian process meets big data: A review of scalable gps. *arXiv preprint arXiv:1807.01065*, 2018.
- [30] A. O’Hagan. Monte carlo is fundamentally unsound. *The Statistician*, pages 247–249, 1987.
- [31] J.-X. Pan and K.-T. Fang. Maximum likelihood estimation. In *Growth curve models and statistical diagnostics*, pages 77–158. Springer, 2002.
- [32] H. Peng, S. Zhe, X. Zhang, and Y. Qi. Asynchronous distributed variational gaussian process for regression. In *Proceedings of the 34th International Conference on Machine Learning-Volume 70*, pages 2788–2797. JMLR. org, 2017.

- [33] J. Quiñero-Candela and C. E. Rasmussen. A unifying view of sparse approximate gaussian process regression. *Journal of Machine Learning Research*, 6(Dec):1939–1959, 2005.
- [34] C. Robert and G. Casella. *Monte Carlo statistical methods*. Springer Science & Business Media, 2013.
- [35] M. Schonlau. *Computer experiments and global optimization*. 1997.
- [36] E. Snelson and Z. Ghahramani. Local and global sparse gaussian process approximations. In *Artificial Intelligence and Statistics*, pages 524–531, 2007.
- [37] C. K. Williams and C. E. Rasmussen. Gaussian processes for machine learning. *the MIT Press*, 2(3):4, 2006.